

Some analytical results for spin 1/2 spin systems. III: The benzene ring

G.J. Bowden, T. Heseltine and M.J. Prandolini

School of Physics, University of New South Wales, Sydney NSW2052, Australia

Received 10 May 1996

In two earlier papers on multiply connected *ABCD* spin 1/2 spin systems, it was shown that it is possible to simplify the calculation of (i) the time dependent density matrix $\rho(t)$, and (ii) the time evolution of high-order multiple quantum operators, evolving in the presence of differing Zeeman offsets, scalar coupling and dipolar interactions, by subdividing the Hamiltonian \mathcal{H} into $(\mathcal{H}_1 + \mathcal{H}_2)$, where \mathcal{H}_1 is a suitable linear combination of the constants of the motion. In this paper, these techniques are applied to the benzene ring with particular emphasis on high-order multiple-quantum NMR experiments, and their interpretation in terms of specific wavefunctions. In particular, it is shown that excellent agreement between theory and experiment can be obtained for the energy splittings witnessed in the $\Delta m = +4, +5$ MQ-NMR transitions, with minimum effort.

1. Introduction

In two preceding papers [1,2], it was shown that the determination of the time dependent density matrix $\rho(t)$, for ABC, etc., coupled spin 1/2 spin systems, can be greatly simplified by subdividing the Hamiltonian into

$$\mathcal{H} = \mathcal{H}_1 + \mathcal{H}_2, \quad (1)$$

where \mathcal{H}_1 commutes with \mathcal{H} . In practice, this is achieved by (i) identifying the constants of the motion for \mathcal{H} , and (ii) setting \mathcal{H}_1 equal to a suitable combination of the constants of the motion. The evolution of the density matrix can then be factorised:

$$\rho(t) = e^{-i\mathcal{H}_2 t/\hbar} \left[e^{-i\mathcal{H}_1 t/\hbar} \rho(0) e^{+i\mathcal{H}_1 t/\hbar} \right] e^{+i\mathcal{H}_2 t/\hbar}. \quad (2)$$

This leads not only to simplifications in the calculation of the density matrix $\rho(t)$, but also in the determination of the eigenvalues and eigenfunctions of \mathcal{H} . In practice, it is a very straight forward matter to compute the evolution of the density matrix under the action of \mathcal{H}_1 , but less so for \mathcal{H}_2 . Nevertheless, even for \mathcal{H}_2 a surprising number of simplifications can be made. For example, (i) if K is the maximum rank tensor available to the spin system, multipolar states of the form

$\rho(0) = \hat{T}_{\pm K}^K$, are simple constants of the motion under the action of \mathcal{H}_2 [1], and (ii) the evolution of high-order tensor operators $\hat{T}_{\pm Q}^K$, where the order $|Q|$ is equal to $K - 1$, requires only a restricted number of eigenfunctions and eigenvalues of \mathcal{H}_2 [2].

In this paper, the techniques developed in [1,2] are applied to the benzene ring, a six spin 1/2 dipolar coupled spin system. The dipole-dipole interactions between the spins are treated within the secular approximation, thus guaranteeing that \mathcal{J}_z is a good quantum number. This observation, together with the sixfold symmetry of the benzene ring itself, is exploited to the full in the determination of the eigenvalues and eigenfunctions of \mathcal{H}_2 .

It should, of course, be noted that in the past the NMR properties of the benzene ring have attracted the attention of many authors, both experimentally and theoretically [3–8]. In particular, the multiple quantum (MQ) NMR spectra of liquid crystal aligned benzene have been well documented, see for example the reviews in [8,9]. However, the treatment given in this paper differs in that (i) it provides analytical solutions for the 64 energy levels and eigenfunctions, (ii) it identifies the wavefunctions targeted in MQ-NMR experiments, and (iii) it provides a simplified framework which can be used to obtain explicit forms for the time evolution of the density matrix $\rho(t)$. In addition, (i) the intuitive comments of [8], concerning the ortho, meta and para descriptions of the MQ-NMR $\Delta m = \pm 4$ transitions, are re-interpreted in the light of the exact solutions, and (ii) although the discussion is confined in the main to $\Delta m \geq 4$ MQ-NMR transitions, the results given in this paper could be extended to discuss all the remaining MQ-transitions, if so desired.

Finally, it should be noted that an exact solution for six dipolar coupled spin 1/2 nuclei, arranged in a C_{2v} symmetry, has been given in [10]. This particular symmetry is encountered in molecules with two rotating methyl groups. Thus the results given in [10] are not applicable to the benzene ring.

2. The benzene ring

As is well known, the benzene ring possesses a sixfold symmetry axis about an axis passing through the centre of the plane, as shown in Fig. 1. However, in the presence of a magnetic field, this symmetry is lowered depending on the number of

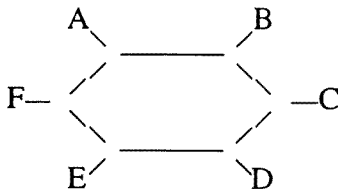


Fig. 1. Labelling scheme used for the benzene ring.

spin-up and spin-down states. In such instances, it is imperative to adhere to a consistent labelling scheme. For the purposes of this paper therefore, we shall use the labelling scheme shown in Fig. 1.

In general, a labelling scheme A, A', ... A''''''', would be more appropriate, to reflect the equivalent nature of all the spins. However, such a labelling scheme is cumbersome.

3. The Hamiltonian

In the secular approximation, the Hamiltonian for the six spin 1/2 hydrogen nuclei associated with the benzene ring can be written in the form

$$\mathcal{H}/\hbar = \sum_i \Delta\omega \mathbf{I}_z(i) + \sum_{i>j} \sum D_{ij} [\mathbf{I}_z(i)\mathbf{I}_z(j) - \frac{1}{4} \{ \mathbf{I}_+(i)\mathbf{I}_-(j) + \mathbf{I}_-(i)\mathbf{I}_+(j) \}], \quad (3)$$

where (i) $\Delta\omega$ is the resonant offset, and (ii) the dipolar constants D_{ij} are given by

$$D_{ij} = \frac{\mu_0\gamma^2}{4\pi\hbar} \left\langle \frac{1 - \cos^2\vartheta_{ij}}{r_{ij}^3} \right\rangle. \quad (4)$$

For this Hamiltonian, the total \mathcal{J}_z operator:

$$\mathcal{J}_z = \sum_i \mathbf{I}_z(i) \quad (7)$$

is a good quantum number. Following [1,2], therefore, it is advantageous to divide the Hamiltonian up into $\mathcal{H}_1 + \mathcal{H}_2$, where (i)

$$\mathcal{H}_1/\hbar = \sum_i \Delta\omega \mathbf{I}_z(i) + \bar{D} \sum_{i>j} \sum \mathbf{I}_z(i)\mathbf{I}_z(j) \quad (8)$$

(ii)

$$\mathcal{H}_2/\hbar = \sum_{i>j} \sum [(D_{ij} - \bar{D})\mathbf{I}_z(i)\mathbf{I}_z(j) - \frac{1}{4} D_{ij} \{ \mathbf{I}_+(i)\mathbf{I}_-(j) + \mathbf{I}_-(i)\mathbf{I}_+(j) \}] \quad (9)$$

and (iii)

$$\bar{D} = \frac{1}{15} \sum_{i>j} \sum D_{ij} = \frac{1}{5} [3D_{12} + 3D_{13} + D_{14}]. \quad (10)$$

Note that for the benzene ring D_{12} , D_{13} , and D_{14} are simply related to each other. However, for the present we shall treat them as independent parameters, until it is imperative to do otherwise.

Using the observation that \mathcal{J}_z is a good quantum number, the 64×64 Hamiltonian matrix for the benzene ring can be block-diagonalized, as shown schematically in Fig. 2. In practice, the Hamiltonian matrix for \mathcal{H}_1 is characterized by

$\mathcal{J}_z =$	3	2	1	0	-1	-2	-3
$\mathcal{H} =$	1 × 1						
		6 × 6					
			15 × 15				
				20 × 20			
					15 × 15		
						6 × 6	
							1 × 1

Fig. 2. Schematic form of the 64×64 matrix for the benzene ring.

simple diagonal entries, in each of the block-diagonal matrices shown in Fig. 2. This is not the case for \mathcal{H}_2 , but it is easily shown that there are null entries in the $|\mathcal{J}_z = \pm 3\rangle$ 1×1 matrices. As a result, multipolar states of the form $\rho(0) = \mathbf{A}_\pm \mathbf{B}_\pm \mathbf{C}_\pm \mathbf{D}_\pm \mathbf{E}_\pm \mathbf{F}_\pm$ (i.e. order $Q = \pm 6$) are constants of the motion under \mathcal{H}_2 , and can only evolve under the action of \mathcal{H}_1 . The precise form of the \mathcal{H}_1 and \mathcal{H}_2 matrices are discussed in more detail in the next two sections.

4. Eigenvalues and eigenvectors of \mathcal{H}_1

In this case it is easily shown that matrix of \mathcal{H}_1 takes the form

$$\begin{aligned} \mathcal{H}_1 = & [+3\Delta\omega + \frac{15}{4}\bar{D}]\mathbf{E}(1) \oplus [+2\Delta\omega + \frac{5}{4}\bar{D}]\mathbf{E}(6) \oplus [+ \Delta\omega - \frac{1}{4}\bar{D}]\mathbf{E}(15) \\ & \oplus [-\frac{3}{4}\bar{D}]\mathbf{E}(20) \\ & \oplus [-\Delta\omega - \frac{1}{4}\bar{D}]\mathbf{E}(15) \oplus [-2\Delta\omega + \frac{5}{4}\bar{D}]\mathbf{E}(6) \oplus [-3\Delta\omega + \frac{15}{4}\bar{D}]\mathbf{E}(1), \quad (11) \end{aligned}$$

where $\mathbf{E}(n)$ is a shorthand for the $n \times n$ unit matrix. The energy levels for \mathcal{H}_1 are shown schematically in Fig. 3. The eigenfunctions and eigenvalues of \mathcal{H}_1 are therefore very transparent.

5. Eigenvalues and eigenvectors of \mathcal{H}_2

The situation for \mathcal{H}_2 is a little more complicated. However, with the definition of \bar{D} of eq. (10), it is easy to show that the $\mathcal{J}_z = \pm 3$ entries in the block diagonal form of \mathcal{H}_2 are identically equal to zero, as mentioned earlier. However, the 6×6 , 15×15 , 20×20 matrices require more attention.

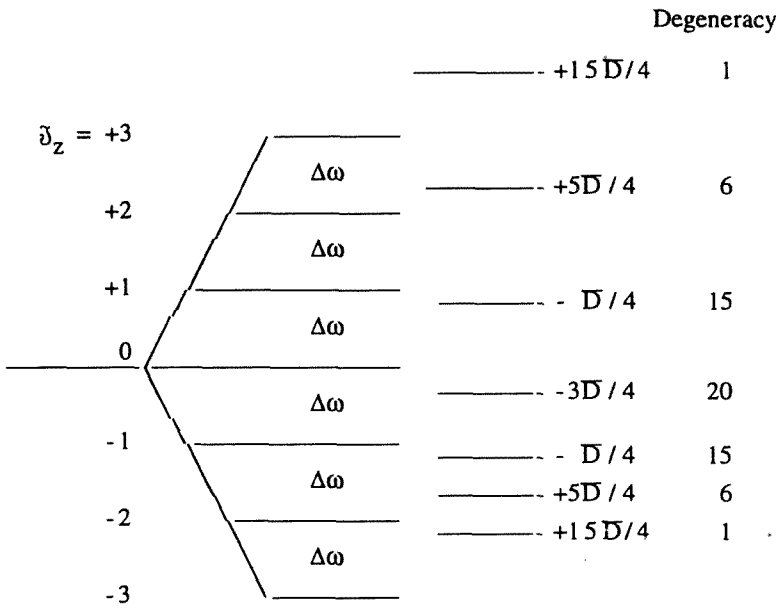


Fig. 3. Energy level diagram for \mathcal{H}_1 .

After some minor algebra, it can be shown that the 6×6 matrix spanned by $\mathcal{J}_z = +2$ (which is identical to that of $\mathcal{J}_z = -2$) is given by

$$\mathcal{H}(\mathcal{J}_z = +2) = -\frac{1}{4} \begin{bmatrix} |A\rangle & |B\rangle & |C\rangle & |D\rangle & |E\rangle & |F\rangle \\ 0 & \alpha & \beta & \gamma & \beta & \alpha \\ \alpha & 0 & \alpha & \beta & \gamma & \beta \\ \beta & \alpha & 0 & \alpha & \beta & \gamma \\ \gamma & \beta & \alpha & 0 & \alpha & \beta \\ \beta & \gamma & \beta & \alpha & 0 & \alpha \\ \alpha & \beta & \gamma & \beta & \alpha & 0 \end{bmatrix}, \quad (12)$$

where (i), for compactness, we have defined

$$\alpha = D_{12},$$

$$\beta = D_{13},$$

$$\gamma = D_{14},$$

$$\bar{D} = \frac{1}{5}(2\alpha + 2\beta + \gamma) \quad (13)$$

and (ii) the 6×6 matrix has been labelled with the wavefunctions $|A\rangle$, $|B\rangle$, $|C\rangle$, $|D\rangle$, $|E\rangle$, $|F\rangle$, where $|X\rangle$ is a shorthand notation for all spins up except at the spin-down position X . Note also that (i) the diagonal terms are zero, and (ii) the 6×6 matrix of (12) is a circulant. The latter is easily diagonalized using the unitary transformation

$$U_6 = \frac{1}{\sqrt{6}} \begin{bmatrix} 1 & 1 & 1 & 1 & 1 & 1 \\ 1 & -1 & 1 & -1 & 1 & -1 \\ 1 & e & e^2 & -1 & e^4 & e^5 \\ 1 & e^5 & e^4 & -1 & e^2 & e \\ 1 & e^2 & e^4 & 1 & e^2 & e^4 \\ 1 & e^4 & e^2 & 1 & e^4 & e^2 \end{bmatrix}, \quad (14)$$

where

$$e = e^{-i2\pi/6}. \quad (15)$$

This unitary transformation reflects the sixfold rotational symmetry of the benzene ring and is identical with the character table for the C_6 group [11]. It is worth noting that (i) this unitary transformation gives equal weighting to the six differing spin configurations used to label (12), and (ii) it leaves the 6×6 matrix of \mathcal{H}_1 , a unit matrix multiplied by the constant $(2\Delta\omega + 5\bar{D}/4)$, unchanged.

With the aid of (14) and (15), we find

$$U_6 \mathcal{H}_2(\mathcal{J}_z = +2) U_6^{-1} = -\frac{1}{4} \begin{bmatrix} (2\alpha + 2\beta + \gamma) & & & & & \\ & (-2\alpha + 2\beta - \gamma) & & & & \mathbf{O} \\ & & (\alpha - \beta - \gamma) & & & \\ & & & (\alpha - \beta - \gamma) & & \\ \mathbf{O} & & & & (-\alpha - \beta + \gamma) & \\ & & & & & (-\alpha - \beta + \gamma) \end{bmatrix}. \quad (16)$$

Thus the energy levels are characterized by two singlets and two doublets. Note also that the leading eigenvalue $E_1 = -(2\alpha + 2\beta + \gamma)/4$ is characterized by the fully symmetric wavefunction

$$|\Psi\rangle_s = \frac{1}{\sqrt{6}}[|A\rangle + |B\rangle + |C\rangle + |D\rangle + |E\rangle + |F\rangle]. \quad (17)$$

This is the wavefunction targeted in a $\Delta m = +5$ multiple quantum experiment, a point first recognized by [6]. Consider the matrix element between the $|\mathcal{J}_z = -3\rangle$ and $|\mathcal{J}_z = +2\rangle$ levels:

$$\text{ME} = \langle \mathcal{J}_z = -3 | \sum_i \mathbf{J}_x(i) | \mathcal{J}_z = +2 \rangle. \quad (18)$$

Since both the operator $\sum \mathbf{J}_x(i)$ and the wavefunction $|\mathcal{J}_z = -3\rangle$ are fully symmetric, only $|\Psi\rangle_s$ of eq. (17) can give a non-zero matrix element ME. Thus of the six possible $\Delta m = +5$ transitions, only one is allowed by symmetry. Further, the energy of this transition is given by

$$\begin{aligned} E[\mathcal{J}_z(-3) \rightarrow \mathcal{J}_z(+2)] &= 5\Delta\omega + [5\bar{D}/4 - \frac{1}{4}(2\alpha + 2\beta + \gamma)] - 15\bar{D}/4 \\ &= 5\Delta\omega - 15\bar{D}/4. \end{aligned} \quad (19)$$

Similarly,

$$E[\mathcal{J}_z(-2) \rightarrow \mathcal{J}_z(+3)] = 5\Delta\omega + 15\bar{D}/4. \quad (20)$$

Thus the $\Delta m = \pm 5$ transition is characterized by two peaks centred on $5\Delta\omega$, with an energy separation of $15\bar{D}/2$. This is indeed found to be the case experimentally. In the case of the benzene ring, therefore, only limited information, in the form of an average dipolar field constant, can be gleaned from $\Delta m = \pm 5$ MQ-transitions. To go further we must examine $\Delta m = \pm 4$ MQ-NMR transitions.

6. Multiple quantum $\Delta m = \pm 4$ transitions

There are three sources of say $\Delta m = +4$ transitions. These are from $|\mathcal{J}_z = -2\rangle \rightarrow |\mathcal{J}_z = +2\rangle$, $|\mathcal{J}_z = -3\rangle \rightarrow |\mathcal{J}_z = +1\rangle$, and $|\mathcal{J}_z = -1\rangle \rightarrow |\mathcal{J}_z = +3\rangle$, respectively. We already have enough information to determine the allowed transitions for the first set of transitions. However, for the remaining two sets of transitions it will be necessary to determine the eigenvalues and eigenvectors of the $|\mathcal{J}_z = \pm 1\rangle$ levels.

In the first place, it is necessary to define our labelling scheme used for the $|\mathcal{J}_z = +1\rangle 15 \times 15 \mathcal{H}_2$ matrix. The first six labels |1> to |6> belong to adjacent down spins i.e. $|AB\rangle$, $|BC\rangle$, $|CD\rangle$, $|DE\rangle$, $|EF\rangle$, $|FA\rangle$. The next six labels |7> to |12> belong to next nearest neighbour down spins i.e.: $|AC\rangle$, $|BD\rangle$, $|CE\rangle$, $|DF\rangle$, $|EA\rangle$, $|FB\rangle$. Finally, the last three labels |13> to |15> belong to those down spins whose separation is a maximum, i.e. $|AD\rangle$, $|BE\rangle$, $|CF\rangle$. Proceeding in this fashion we find the $|\mathcal{J}_z = +1\rangle \mathcal{H}_2$ matrix:

$$\mathcal{H}_2(\mathcal{J}_z = +1) = (-1/4) \times$$

η	β	0	0	0	β	α	γ	0	0	γ	α	β	β	0
β	η	β	0	0	0	α	α	γ	0	0	γ	0	β	β
0	β	η	β	0	0	γ	α	α	γ	0	0	β	0	β
0	0	β	η	β	0	0	γ	α	α	γ	0	β	β	0
0	0	0	β	η	β	0	0	γ	α	α	γ	0	β	β
β	0	0	0	β	η	γ	0	0	γ	α	α	β	0	β
α	α	γ	0	0	γ	χ	0	β	0	β	0	α	0	α
γ	α	α	γ	0	0	0	χ	0	β	0	β	α	α	0
0	γ	α	α	γ	0	β	0	χ	0	β	0	0	α	α
0	0	γ	α	α	γ	0	β	0	χ	0	β	α	0	α
γ	0	0	γ	α	α	β	0	β	0	χ	0	α	α	0
α	γ	0	0	γ	α	0	β	0	β	0	χ	0	α	α
β	0	β	β	0	β	α	α	0	α	α	0	ξ	0	0
β	β	0	β	β	0	0	α	α	0	α	α	0	ξ	0
0	β	β	0	β	β	α	0	α	α	0	α	0	0	ξ

(21)

where the three new diagonal symbols η , χ , and ξ are given by

$$\begin{aligned} \eta &= -4[(2\alpha - 2\beta - \gamma)/4 + \bar{D}/4] = 4[\bar{D} - \alpha], \\ \chi &= -4[(-2\alpha + 2\beta - \gamma)/4 + \bar{D}/4] = 4[\bar{D} - \beta], \\ \xi &= -4[(-2\alpha - 2\beta + 3\gamma)/4 + \bar{D}/4] = 4[\bar{D} - \gamma]. \end{aligned} \tag{22}$$

Note that (i) while the partitioned matrices are in themselves circulants, the overall matrix is not, and (ii) the term $4\bar{D}$ is common to all the diagonal elements and can therefore be extracted as a common energy shift.

To block-diagonalize (21), we make use of the unitary transformation of (14) twice, together with a new 3×3 unitary transformation appropriate to C_3 symmetry, i.e.

$$U = U_6 \oplus U_6 \oplus U_3, \tag{23}$$

where

$$U_3 = \frac{1}{\sqrt{3}} \begin{bmatrix} 1 & 1 & 1 \\ 1 & \omega & \omega^* \\ 1 & \omega^* & \omega \end{bmatrix} \quad (\omega = e^{-i2\pi/3}). \tag{24}$$

The required transformation was performed using Mathematica together with eq. (21) with the common energy denominator $-\bar{D}$ removed. With this symmetry

transformation, it was found that the number of non-zero entries in 15×15 matrix of (21) was reduced from 135 to 37. Further, the new 37 entries could be block-diagonalized according to

$$\mathcal{H}(\mathcal{J}_z = +1)/\hbar = -\bar{D} - \frac{1}{4}[\mathbb{H}_1 \oplus \mathbb{H}_2 \oplus \mathbb{H}_3 \oplus \mathbb{H}_4 \oplus \mathbb{H}_5 \oplus \mathbb{H}_6 \oplus \mathbb{H}_7], \quad (25)$$

where

$$\mathbb{H}_1 = \begin{array}{ccc} 1' & 7' & 13' \\ \begin{array}{|ccc|} \hline -4\alpha + 2\beta & 2(\alpha + \gamma) & 2\beta\sqrt{2} \\ 2(\alpha + \gamma) & -2\beta & 2\alpha\sqrt{2} \\ 2\beta\sqrt{2} & 2\alpha\sqrt{2} & -4\gamma \\ \hline \end{array} & , & \mathbb{H}_2 = \begin{array}{c} 2' \\ \begin{array}{|c|} \hline -4\alpha - 2\beta \\ \hline \end{array} \end{array}$$

$$\mathbb{H}_3 = \begin{array}{cc} 3' & 9' \\ \begin{array}{|cc|} \hline -4\alpha + \beta & z_1\alpha \\ z_1^*\alpha & -5\beta \\ \hline \end{array} \end{array}$$

$$\mathbb{H}_4 = \begin{array}{cc} 4' & 10' \\ \begin{array}{|cc|} \hline -4\alpha + \beta & z_1^*\alpha \\ z_1\alpha & -5\beta \\ \hline \end{array} & , \quad z_1 = \left(\frac{3}{2} + i\frac{\sqrt{3}}{2} \right)$$

$$\mathbb{H}_5 = \begin{array}{ccc} 5' & 11' & 14' \\ \begin{array}{|ccc|} \hline -4\alpha - \beta & z_2(\alpha - 2\gamma) & \sqrt{2}z_2^*\beta \\ z_2^*(\alpha - 2\gamma) & -5\beta & \sqrt{2}z_2\alpha \\ \sqrt{2}z_2\beta & \sqrt{2}z_2^*\alpha & -4\gamma \\ \hline \end{array} & , & z_2 = \left(\frac{1}{2} + i\frac{\sqrt{3}}{2} \right)$$

$$\mathbb{H}_6 = \begin{array}{ccc} 6' & 12' & 15' \\ \begin{array}{|ccc|} \hline -4\alpha - \beta & z_2^*(\alpha - 2\gamma) & \sqrt{2}z_2\beta \\ z_2(\alpha - 2\gamma) & -5\beta & \sqrt{2}z_2^*\alpha \\ \sqrt{2}z_2^*\beta & \sqrt{2}z_2\alpha & -4\gamma \\ \hline \end{array} \end{array}$$

$$\mathbb{H}_7 = \begin{array}{c} 8' \\ \begin{array}{|c|} \hline -2\beta \\ \hline \end{array} \end{array} \quad (26)$$

Note that the labels are now $|1'\rangle, |2'\rangle$, etc., to reflect the new wavefunctions obtained following the unitary transformation of (23).

From an examination of (26), it is clear that the original 15×15 matrix has been

block-diagonalized into three 3×3 , two, 2×2 , and two 1×1 matrices. Thus the problem of diagonalizing the $|\mathcal{J}_z = +1\rangle 15 \times 15$ matrix of \mathcal{H}_2 has been reduced considerably. Secondly, we note that the three wavefunctions of \mathbb{H}_1 are completely symmetric, being spanned by the wavefunctions $|1'\rangle$, $|7'\rangle$, $|13'\rangle$. It is these wavefunctions which are the eigenvectors targeted in $\Delta m = +4$ MQ-experiments via the matrix elements:

$$\text{ME} = \langle \mathcal{J}_z = -3 | \sum_i \mathbf{J}_x(i) | \mathcal{J}_z = +1 \rangle. \quad (27)$$

As a result, symmetry considerations dictate that the number of $\Delta m = +4$ MQ-NMR transitions emanating from $|\mathcal{J}_z = -3\rangle$ to $|\mathcal{J}_z = +1\rangle$ is limited to a maximum of 3. In general, of course, analytical solutions for the 3×3 matrix \mathbb{H}_1 , can be found. However, when expressed in terms of α , β , and γ , these are rather tedious. Instead therefore, we have calculated the eigenvalues of \mathbb{H}_1 by setting $\beta = \alpha/(3\sqrt{3})$ and $\gamma = \alpha/8$, and subsequently re-expressing the eigenvalues in terms of \bar{D} . We find $(-9.91406\bar{D}, +5.9854\bar{D}, -5.03584\bar{D})$ for the 3×3 matrix of \mathbb{H}_1 . Thus the eigenvalues of the \mathcal{H}_2 3×3 matrix, associated with the three symmetric wavefunctions $|1'\rangle$, $|7'\rangle$, $|13'\rangle$, are given by $(1.47851\bar{D}, -2.49635\bar{D}, -0.25896\bar{D})$. In summary, therefore, the three transitions from $|\mathcal{J}_z = -3\rangle \rightarrow |\mathcal{J}_z = +1\rangle$ are given by

$$\begin{aligned} \Delta E_1 &= 4\Delta\omega - 4\bar{D} + 1.47851\bar{D}, \\ \Delta E_2 &= 4\Delta\omega - 4\bar{D} + 0.25896\bar{D}, \\ \Delta E_3 &= 4\Delta\omega - 4\bar{D} - 2.49635\bar{D}. \end{aligned} \quad (28)$$

Likewise, for the $|\mathcal{J}_z = -1\rangle \rightarrow |\mathcal{J}_z = +3\rangle$ transitions:

$$\begin{aligned} \Delta E_1 &= 4\Delta\omega + 4\bar{D} - 1.47851\bar{D}, \\ \Delta E_2 &= 4\Delta\omega + 4\bar{D} - 0.25896\bar{D}, \\ \Delta E_3 &= 4\Delta\omega + 4\bar{D} + 2.49635\bar{D}. \end{aligned} \quad (29)$$

Finally, of course, we must add the $\Delta m = +4$ MQ-NMR transitions emanating from $|\mathcal{J}_z = -2\rangle$ to $|\mathcal{J}_z = +2\rangle$. Using the eigenfunctions, obtained using the unitary transformation of (13), it is easily shown that there are 6 allowed transitions of this nature. However, all of these transitions possess the same energy $4\Delta\omega$. In summary, therefore, we expect one peak at $4\Delta\omega$, flanked symmetrically by three lines below $4\Delta\omega$, and three lines above $4\Delta\omega$. This is found to be the case experimentally, with the transition at $4\Delta\omega$ being the strongest. However, it should be noted that the intensities of the transitions are governed not only by matrix elements of the form (27), but also by the nature of the high-rank multipolar state formed in a MQ-NMR experiment [9,12].

We are now in a position to make contact with experiment. From the MQ-NMR results of [6], the splitting between the two $\Delta m = 5$ peaks is 3.23(5) kHz. Since this splitting is given by $7.5\bar{D}$, we therefore deduce that $\bar{D} = 0.431(7)$ kHz. This result can then be used to predict the energy splittings between the $\Delta m = +4$ transitions. For the two outermost $\Delta m = +4$ peaks, the energy separation should be $12.9927\bar{D}$ or 5.6(1) kHz, which compares very favourably with the measured value of 5.7(1) kHz. The predictions for the two other pairs of peaks are 3.22(5) kHz ($= 7.48208\bar{D}$) and 2.17(4) kHz ($= 5.0298\bar{D}$), which are to be compared with the measured separations of 3.23(6) kHz and 2.16(4) kHz, respectively. Clearly, there is a good agreement between theory and experiment.

Finally, before closing this section we make two further points. Firstly, the eigenvalues of \mathbb{H}_3 and \mathbb{H}_4 are identical, as are those of \mathbb{H}_5 and \mathbb{H}_6 . Thus in practice, it is only necessary to diagonalize two 3×3 and one 2×2 matrices to obtain a full solution for the 15×15 $\mathcal{J}_z = 1$ matrix of \mathcal{H}_2 . Secondly, it has been suggested that the three pairs of peaks witnessed experimentally in the benzene $\Delta m = \pm 4$ MQ-NMR experiment are associated with the “down-spins” being placed in the para, meta, and ortho-positions around the benzene ring. Since the dipolar energies of these three spin-configurations differ, we have a natural way of explaining the three observed transitions. However, in practice the situation is a little more complicated. From an examination of \mathbb{H}_1 it is clear that the eigenfunctions take the form

$$\Psi = a_j|1'\rangle + b_j|7'\rangle + c_j|13'\rangle \quad (j = 1 - 3). \quad (30)$$

where (i) a_j , b_j and c_j are numerical coefficients obtained by diagonalizing \mathbb{H}_1 , and (ii) the wavefunctions $|1'\rangle$, etc., are shorthand notations for

$$\begin{aligned} |1'\rangle &= \frac{1}{\sqrt{6}}[|AB\rangle + |BC\rangle + |CD\rangle + |DE\rangle + |EF\rangle + |FA\rangle] \quad (\text{para}), \\ |7'\rangle &= \frac{1}{\sqrt{6}}[|AC\rangle + |BD\rangle + |CE\rangle + |DF\rangle + |EA\rangle + |FB\rangle] \quad (\text{meta}), \\ |13'\rangle &= \frac{1}{\sqrt{3}}[|AD\rangle + |BE\rangle + |CF\rangle] \quad (\text{ortho}). \end{aligned} \quad (31)$$

Thus in practice, the eigenfunctions are characterized by three distinct mixtures of the para, meta and ortho spin configurations for the $|\mathcal{J}_z = +1\rangle$ state, rather than the three para, meta, and ortho states taken separately.

7. The $\mathcal{J}_z = 0$ 20×20 matrix

For completeness, the block-diagonalization of the 20×20 $|\mathcal{J}_z = 0\rangle$ matrix is detailed in this section, although we shall not give a full discussion of the $\Delta m = \pm 3$ or lower MQ-NMR transitions.

The matrix in question can be partitioned in the following form:

$$\mathcal{H}(\mathcal{J}_z = 0) = -\frac{1}{4} \begin{bmatrix} \mathbf{A}_{11} & \mathbf{A}_{12} & \mathbf{A}_{13} & \mathbf{A}_{14} \\ \mathbf{A}_{12}^\dagger & \mathbf{A}_{22} & \mathbf{A}_{23} & \mathbf{A}_{24} \\ \mathbf{A}_{13}^\dagger & \mathbf{A}_{23}^\dagger & \mathbf{A}_{33} & \mathbf{A}_{34} \\ \mathbf{A}_{14}^\dagger & \mathbf{A}_{24}^\dagger & \mathbf{A}_{34}^\dagger & \mathbf{A}_{44} \end{bmatrix}, \tag{32}$$

where the individual matrices, which are circulants, are given in Table 1, together with their labelling schemes. The unitary transform which reduces the 20×20 $\mathcal{J}_z = 0$ matrix to block-diagonal form is given by

$$\mathbf{U} = \mathbf{U}_6 \oplus \mathbf{U}_6 \oplus \mathbf{U}_6 \oplus \mathbf{U}_2, \tag{33}$$

where the \mathbf{U}_6 matrices are given by eq. (14), and the new 2×2 matrix \mathbf{U}_2 by

$$\mathbf{U}_2 = \sqrt{\frac{1}{2}} \begin{bmatrix} 1 & 1 \\ 1 & -1 \end{bmatrix}. \tag{34}$$

After performing the unitary transformation, it is easily shown that the $\mathcal{J}_z = 0$ matrix takes the form

$$\mathcal{H}_2(\mathcal{J}_z = +0)/\hbar = -\frac{3}{4} \bar{D}E(20) - \frac{1}{4} [\mathbb{H}'_1 \oplus \mathbb{H}'_2 \oplus \mathbb{H}'_3 \oplus \mathbb{H}'_4 \oplus \mathbb{H}'_5 \oplus \mathbb{H}'_6], \tag{35}$$

where

$$\mathbb{H}'_1 = \begin{array}{c} \begin{array}{cccc} 1' & 7' & 13' & 19' \\ \hline -8\alpha + 8\beta + 14\gamma & \alpha + 2\beta & \alpha + 2\beta & \sqrt{3}\gamma \\ \alpha + 2\beta & 8\alpha + 8\beta - 3\gamma & 2(\alpha + \beta) & \sqrt{3}\alpha \\ \alpha + 2\beta & 2(\alpha + \beta) & 8\alpha + 8\beta - 3\gamma & \sqrt{3}\alpha \\ \sqrt{3}\gamma & \sqrt{3}\alpha & \sqrt{3}\alpha & 12(2\alpha - 2\beta - \gamma) \end{array} \end{array}$$

$$\mathbb{H}'_2 = \begin{array}{c} \begin{array}{cccc} 2' & 8' & 14' & 20' \\ \hline -8\alpha + 8\beta + 10\gamma & \alpha - 2\beta & -\alpha + 2\beta & \sqrt{3}\gamma \\ \alpha - 2\beta & 8\alpha + 8\beta - 5\gamma & 2(\alpha - \beta) & -\sqrt{3}\alpha \\ -\alpha + 2\beta & 2(\alpha - \beta) & 8\alpha + 8\beta - 5\gamma & \sqrt{3}\alpha \\ \sqrt{3}\gamma & -\sqrt{3}\alpha & \sqrt{3}\alpha & 12(2\alpha - 2\beta - \gamma) \end{array} \end{array}$$

$$\mathbb{H}'_3 = I' \begin{array}{c} \begin{array}{ccc} 3' & 9' & 15' \\ \hline -8\alpha + 8\beta + 13\gamma & \alpha + \beta & z(\alpha + \beta) \\ \alpha + \beta & 8\alpha + 8\beta - 5\gamma & z(\alpha - \beta) \\ z^*(\alpha + \beta) & z^*(\alpha - \beta) & 8\alpha + 8\beta - 5\gamma \end{array} \end{array} \quad z = \frac{1}{2}(1 + i\sqrt{3})$$

Table 1

Partitioned matrices for the $\mathcal{J}_z = 020 \times 20$ matrix.

$$A_{11} = \begin{pmatrix} ABC & BCD & CDE & DEF & EFA & FAB \\ \Psi & \gamma & 0 & 0 & 0 & \gamma \\ \gamma & \Psi & \gamma & 0 & 0 & 0 \\ 0 & \gamma & \Psi & \gamma & 0 & 0 \\ 0 & 0 & \gamma & \Psi & \gamma & 0 \\ 0 & 0 & 0 & \gamma & \Psi & \gamma \\ \gamma & 0 & 0 & 0 & \gamma & \Psi \end{pmatrix}; \quad A_{22} = \begin{pmatrix} ABC & BCE & CDF & DEA & EFB & FAC \\ \Phi & 0 & 0 & \gamma & 0 & 0 \\ 0 & \Phi & 0 & 0 & \gamma & 0 \\ 0 & 0 & \Phi & 0 & 0 & \gamma \\ \gamma & 0 & 0 & \Phi & 0 & 0 \\ 0 & \gamma & 0 & 0 & \Phi & 0 \\ 0 & 0 & \gamma & 0 & 0 & \Phi \end{pmatrix}$$

$$A_{33} = \begin{pmatrix} ACD & BDE & CEF & DFA & EAB & FBC \\ \Phi & 0 & 0 & \gamma & 0 & 0 \\ 0 & \Phi & 0 & 0 & \gamma & 0 \\ 0 & 0 & \Phi & 0 & 0 & \gamma \\ \gamma & 0 & 0 & \Phi & 0 & 0 \\ 0 & \gamma & 0 & 0 & \Phi & 0 \\ 0 & 0 & \gamma & 0 & 0 & \Phi \end{pmatrix}; \quad A_{44} = \begin{pmatrix} ACE & BDF \\ \Delta & 0 \\ 0 & \Delta \end{pmatrix},$$

$$A_{12} = \begin{pmatrix} ABD & BCE & CDF & DEA & EFB & FAC \\ ABC & \alpha & \beta & 0 & 0 & \beta \\ BCD & \beta & \alpha & \beta & 0 & 0 \\ CDE & 0 & \beta & \alpha & \beta & 0 \\ DEF & 0 & 0 & \beta & \alpha & \beta \\ EFA & 0 & 0 & 0 & \beta & \alpha \\ FAB & \beta & 0 & 0 & 0 & \alpha \end{pmatrix}; \quad A_{13} = \begin{pmatrix} ACD & BDE & CEF & DFA & EAB & FBC \\ ABC & \alpha & \beta & 0 & 0 & \beta \\ BCD & \beta & \alpha & \beta & 0 & 0 \\ CDE & 0 & \beta & \alpha & \beta & 0 \\ DEF & 0 & 0 & \beta & \alpha & \beta \\ EFA & 0 & 0 & 0 & \beta & \alpha \\ FAB & \beta & 0 & 0 & 0 & \alpha \end{pmatrix}$$

$$A_{23} = \begin{pmatrix} ACD & BDE & CEF & DFA & EAB & FBC \\ ABD & \alpha & \beta & 0 & \beta & \alpha \\ BCE & 0 & \alpha & \beta & 0 & \alpha \\ CDF & \alpha & 0 & \alpha & \beta & \beta \\ DEA & \beta & \alpha & 0 & \alpha & 0 \\ EFB & 0 & \beta & \alpha & 0 & \beta \\ FAC & \beta & 0 & \beta & \alpha & \alpha \end{pmatrix}$$

$$A_{14} = \begin{pmatrix} ACE & BDF \\ ABD & \gamma & 0 \\ BCD & 0 & \gamma \\ CDE & \gamma & 0 \\ DEF & 0 & \gamma \\ EFA & \gamma & 0 \\ FAB & 0 & \gamma \end{pmatrix}; \quad A_{24} = \begin{pmatrix} ACE & BDF \\ ABD & 0 & \alpha \\ BCE & \alpha & 0 \\ CDF & 0 & \alpha \\ DEA & \alpha & 0 \\ EFB & 0 & \alpha \\ FAC & \alpha & 0 \end{pmatrix}; \quad A_{34} = \begin{pmatrix} ACE & BDF \\ ACD & \alpha & 0 \\ BDE & 0 & \alpha \\ CEF & \alpha & 0 \\ DFA & 0 & \alpha \\ EAB & \alpha & 0 \\ FBC & 0 & \alpha \end{pmatrix}$$

Key: $\Psi = -4(2\alpha - 2\beta - 3\gamma)$, $\Phi = -4(-2\alpha - 2\beta + \gamma)$, $\Delta = -4(-6\alpha + 6\beta - 3\gamma)$

$$\mathbb{H}'_4 = \begin{array}{c} \begin{array}{ccc} 4' & 10' & 16' \\ \hline -8\alpha + 8\beta + 13\gamma & \alpha + \beta & z^*(\alpha + \beta) \\ \alpha + \beta & 8\alpha + 8\beta - 5\gamma & z^*(\alpha - \beta) \\ z(\alpha + \beta) & z(\alpha - \beta) & 8\alpha + 8\beta - 5\gamma \end{array} \end{array}$$

$$\mathbb{H}'_5 = \begin{array}{c} \begin{array}{ccc} 5' & 11' & 17' \\ \hline -8\alpha + 8\beta + 11\gamma & \alpha - \beta & z^*(-\alpha + \beta) \\ \alpha - \beta & 8\alpha + 8\beta - 3\gamma & z^*(\alpha + \beta) \\ z(-\alpha + \beta) & z(\alpha + \beta) & 8\alpha + 8\beta - 3\gamma \end{array} \end{array}$$

$$\mathbb{H}'_6 = \begin{array}{c} \begin{array}{ccc} 6' & 12' & 18' \\ \hline -8\alpha + 8\beta + 11\gamma & \alpha - \beta & z(-\alpha + \beta) \\ \alpha - \beta & 8\alpha + 8\beta - 3\gamma & z(\alpha + \beta) \\ z^*(-\alpha + \beta) & z^*(\alpha + \beta) & 8\alpha + 8\beta - 3\gamma \end{array} \end{array}$$

Note that the labelling scheme 1'–20' used in (36) implies that the new wavefunctions are those obtained after applying the unitary transformation of (33).

From an examination of (35) and (36), it is evident that the 20×20 $\mathcal{J}_z = 0$ matrix has been block-diagonalized into two 4×4 matrices and four 3×3 matrices. Further, the eigenvalues of \mathbb{H}_3 are identical to those for \mathbb{H}_4 , as are those for \mathbb{H}_5 and \mathbb{H}_6 . Thus even for the 20×20 $\mathcal{J}_z = 0$ matrix, it is only really necessary to diagonalize two 4×4 matrices, and two 3×3 matrices. Finally, we note that since there are only four symmetric eigenfunctions belonging to \mathbb{H}_1 , this limits the allowed transitions from $|\mathcal{J}_z = -3\rangle \rightarrow |\mathcal{J}_z = 0\rangle$ to just four, with a similar result for the $|\mathcal{J}_z = 0\rangle \rightarrow |\mathcal{J}_z = +3\rangle$ transitions. To these, of course, we must add the allowed transitions from $|\mathcal{J}_z = -2\rangle \rightarrow |\mathcal{J}_z = 1\rangle$, and $|\mathcal{J}_z = -1\rangle \rightarrow |\mathcal{J}_z = 2\rangle$.

8. Conclusions

In this paper, it has been shown that analytical solutions can be obtained for the evolution of the six spin 1/2 dipolar coupled hydrogen nuclei of the benzene ring, in the secular approximation. This has been proved possible by (i) exploiting the fact that \mathcal{J}_z is a good quantum number, (ii) dividing the Hamiltonian up into two commuting terms $\mathcal{H}_1 + \mathcal{H}_2$, and (iii) devising unitary transformations which exploit the symmetry of the benzene ring, reduced by differing combinations of spin-up and spin-down spins. The results have allowed clear identification of (i) the allowed $\Delta m = \pm 4, 5$, and 6 MQ-NMR transitions, and (ii) the initial and final

wavefunctions involved in such transitions. Finally, the origins of the $\Delta m = +4$ $|\mathcal{J}_z = -3\rangle|\mathcal{J}_z = +1\rangle$, and $|\mathcal{J}_z = -1\rangle|\mathcal{J}_z = +3\rangle$ MQ-NMR transitions have been discussed in the light of the exact solutions. In particular, it has been demonstrated that the three pairs of transitions either side of $4\Delta\omega$ central peak are characterized by differing mixtures of the para, meta, and ortho spin configurations. Finally, it has been shown that there is an excellent agreement between theory and experiment for the energy splittings of the $\Delta m = +4$ and $+5$ MQ-NMR transitions.

References

- [1] G.J. Bowden and T. Heseltine, *J. Math. Chem.* 19 (1996) 353.
- [2] G.J. Bowden, T. Heseltine and M.J. Prandolini, *J. Math. Chem.* 19 (1996) 365.
- [3] W.S. Warren, S. Sinton, D.P. Weitekamp and A. Pines, *Phys. Rev. Lett.* 43 (1979) 1791.
- [4] W.S. Warren, Ph.D. Thesis, Berkeley (1980).
- [5] W.S. Warren and A. Pines, *J. Chem. Phys.* 74 (1981) 2808.
- [6] W.S. Warren and A. Pines, *J. Am. Chem. Soc.* 103 (1981) 1613.
- [7] G. Drobny, A. Pines, S. Sinton, W.S. Warren and D.P. Weitekamp, *Phil. Trans. Roy. Soc. London A* 299 (1981) 585.
- [8] A. Pines, Lectures on Pulsed NMR, *Proc. 100th Fermi School of Physics*, Varenna, Italy (1986).
- [9] M. Mehring, *Principles of High Resolution NMR in Solids* (Springer, Berlin Heidelberg, New York, 1983).
- [10] A.M. Panich, *J. Mag. Reson.* 66 (1986) 9.
- [11] M. Tinkham, *Group Theory and Quantum Mechanics* (McGraw-Hill, 1964).
- [12] R.R. Ernst, G. Bodenhausen and A. Wokaun, *Principles of Nuclear Magnetic Resonance in One and Two Dimensions* (Clarendon Press, Oxford, 1987).